Amine-Based Interfacial Molecules for Inverted Polymer-Based Optoelectronic Devices

Bo Ram Lee, Seungjin Lee, Jong Hyun Park, Eui Dae Jung, Jae Choul Yu, Yun Seok Nam, Jinhee Heo, Ju-Young Kim, Byeong-Su Kim, and Myoung Hoon Song**

Over the past few decades, polymer-based light-emitting diodes (PLEDs) and organic solar cells (OSCs) have been intensively investigated because of their advantages, which include cost-effective and large-area fabrication via simple solution-processing as well as flexible mechanical properties.[1–8] However, OSCs and PLEDs for commercial applications require highly efficient device performance and stability. Conventional structured devices with low-work-function (WF) electrodes such as calcium, lithium fluoride (LiF), and aluminum exhibit highly efficient device performance but inferior device stability and operating lifetime.[9,10] Thus, strict encapsulation is required to prevent degradation due to oxygen and moisture.[11] Conversely, inverted-structure devices with high-WF electrodes such as silver and gold as an anode, a metal oxide such as zinc oxide (ZnO) as an electron injection/extraction layer (EIL/EEL) and molybdenum oxide (MoO_3) as a hole injection/extraction layer (HIL/HEL) are promising devices for excellent device stability.[10,12–18] Various approaches have improved device performance through device optimization; these approaches include interfacial engineering/surface modification[19–32] and synthesis of effective active materials with a high quantum yield.[33–40] Interface engineering is suggested to solve the intrinsic limitation of unbalanced charge injection in inverted PLEDs (iPLEDs) and charge extraction in inverted OSCs (iOSCs). Balanced charge injection or extraction is very important for highly efficient iPLEDs and iOSCs, which is caused by well-matched energy levels between the EIL/EEL and the active layer.

The hole injection is effective because of the formation of Ohmic contact at the interface between the MoO_3 and the active layer,[41,42] whereas the electrons injection is inefficient because of a larger energy gap between the conduction band (CB) of metal-oxide and the lowest unoccupied molecular orbital (LUMO) of the active layers in iPLEDs.[14,19,21,23,27,28,30–32] iPLEDs have a large energy barrier of ≈1.6 eV at the interface between the LUMO of super yellow (SY, ≈2.7 eV)[14,21] and the CB of ZnO (≈4.3 eV), which requires a minimized difference of energy levels for excellent electron injection. However, the difference among the energy levels of iOSC devices for excellent electron extraction is relatively lower (≈0.3 eV) at the interface between the CB of ZnO and the LUMO of [6,6]-phenyl-C_{71}-butyric acid methyl ester ($PC_{71}BM$) as an electron-acceptor material (≈4.0 eV)[43–45] compared to the corresponding difference in an iPLED device.

In addition, interfacial engineering influences the reduction of interfacial resistance and the passivation of defect sites, which enhances device performance by reducing the leakage current.[46–50] The use of interfacial engineering can also improve the blocking behaviors of abundant holes, which increase the recombination probability of electron holes in a PLED device[14,22,23,27,31] while suppressing the bimolecular recombination by photogenerated holes and electrons in a OSC device.[32,51–53]

Previous established methods of interfacial engineering, such as ionic liquid molecules (ILMs),[21] conjugated polyelectrolytes (CPEs),[22–24,29] and polymers that contain aliphatic amine groups,[25–28] require expensive and complex synthesis processing. They are unable to easily control the desired energy levels at the interface between the ZnO and the active layer according to the device configuration, such as iPLEDs and iOSCs.

In this Communication, we present a new interfacial engineering method by introducing a series of amine-based interfacial molecules (AIMs) that contain 2 to 6 amine groups (2 to 6N) for highly efficient iPLED and iOSC devices. Our method provides simple and efficient processing and effective tunability of the energy level at the interface between the ZnO and the active layer, depending on the number of amine groups. We investigate the effect of the number of amine groups of one solvent molecule on the tunability of the energy barrier by fixing the total number of amine groups in AIMs solutions. Different concentrations of amine groups are used in iPLEDs (0.30 M) and iOSCs (0.06 M) for optimized device performance. In general, thicker interfacial layer is required for higher device performance in iPLEDs because thicker interfacial layer effectively blocks hole carriers and reduces exciton quenching at the interface between ZnO dand emissive layer.[27,31] On the other hand, thinner interfacial layer is more suitable for efficient charge extraction from active layer to the ZnO in iOSCs.[32]

As the number of amine groups increases, the WFs of AIMs-modified ZnO gradually shift toward the vacuum level from 0.2 eV (2N) to 0.5 eV (6N) compared with the WF of intrinsic ZnO. This finding suggests that AIMs can easily control the

Dr. B. R. Lee, S. Lee, J. H. Park, E. D. Jung, J. C. Yu, Y. S. Nam, Prof. J.-Y. Kim, Prof. M. H. Song
Depart of Materials Science and Engineering and KIST-UNIST Ulsan Center for Convergent Materials
Ulsan National Institute of Science and Technology (UNIST)
UNIST-gil 50, Ulsan 689-798, South Korea
E-mail: mhsong@unist.ac.kr
Dr. J. Heo
Korea Institute of Materials Science (KIMS)
#797 Changwondaero, Changwon, Gyeongnam 641-831, South Korea
Prof. B.-S. Kim
Department of Chemistry and Department of Energy Engineering
Ulsan National Institute of Science and Technology (UNIST)
UNIST-gil 50, Ulsan 689-798, South Korea
E-mail: bskim19@unist.ac.kr

DOI: 10.1002/adma.201500663

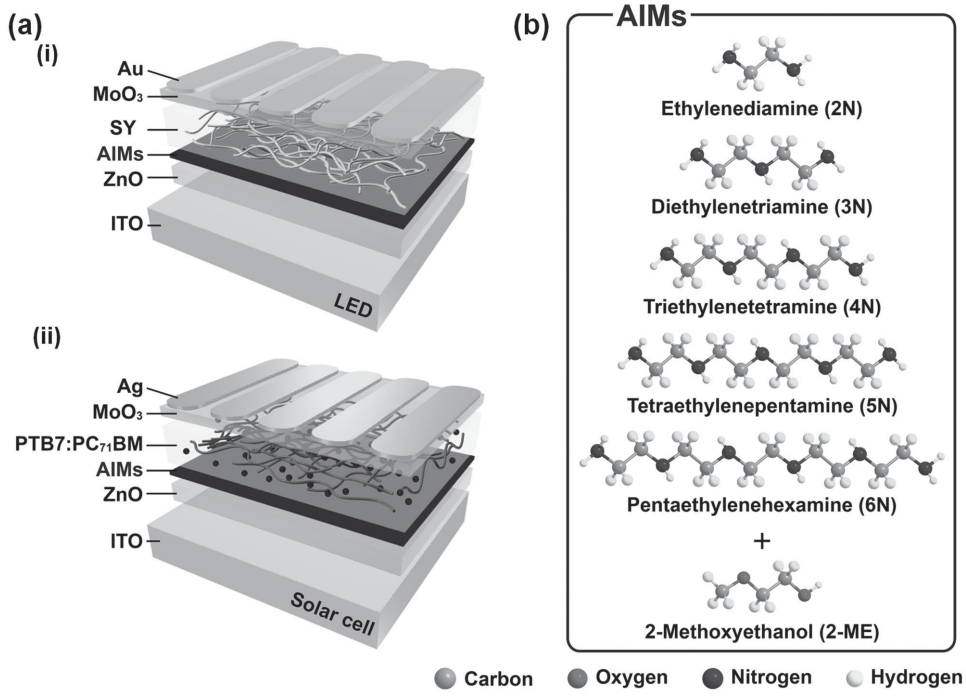

Figure 1. Schematic of iPLED and iOSC devices and chemical structures of AIMs. a) Device architectures of iPLED and iOSC. b) Chemical structures of AIMs, such as ethylenediamine (EDA, 2N), diethylenetriamine (DETA, 3N), triethylenetetramine (TETA, 4N), tetraethylenepentamine (TEPA, 5N), and pentaethylenehexamine (PEHA, 6N) with 2-methoxyethanol (2-ME).

desired energy level to achieve the maximum device performance in iPLEDs and iOSCs. We discovered that AIMs treatment reduces the leakage current and improves the hole-blocking behavior by passivation of defect sites on the ZnO surface, which improves device performance.

Figure 1 represents the device architectures of iPLEDs and iOSCs and the chemical structures of AIMs such as ethylenediamine (EDA, 2N), diethylenetriamine (DETA, 3N), triethylenetetramine (TETA, 4N), tetraethylenepentamine (TEPA, 5N), and pentaethylenehexamine (PEHA, 6N); 2-methoxyethanol (2-ME) was used as a control. Both devices are composed of indium tin oxide (ITO) as a transparent cathode, ZnO as an EIL/EEL, an AIM as an interfacial layer, MoO_3 as a HIL/HEL, and Au and Ag as a metal anode in iPLEDs and iOSCs, respectively. Each solvent bears a different number of amine groups and ethylene groups, ranging from 2 (EDA) to 6 (PEHA), as shown in Figure 1b. The chemical structures of SY, poly[[4,8-bis[(2-ethylhexyl)oxy]benzo[1,2-b:4,5-b′]dithiophene-2,6-diyl][3-fluoro-2-[(2-ethylhexyl)carbonyl]thieno[3,4-b]thiophenediyl]] (PTB7, 1-material, Inc.), and $PC_{71}BM$ are illustrated (see Figure S1, Supporting Information).

The current density and luminance versus voltage (*J*–*V*–*L*) and the device efficiencies of iPLEDs with and without AIMs are shown in **Figure 2**a–d. The current densities of iPLEDs with AIMs are significantly lower than the current densities of the reference device at low voltages (Figure 2a), which indicates that AIMs reduces the leakage current by the passivation of defect sites on the ZnO surface.

Figure 3, Figure S2 and Table S1, Supporting Information, provide evidence for the passivation of defect sites on the ZnO surface via the analysis of time-correlated single photon counting (TCSPC) and photoluminescence (PL). The time-resolved PL signals and PL spectra of SY showed that exciton lifetimes and PL intensities of quartz/ZnO/AIMs/SY were higher than those of quartz/ZnO/SY, which indicates that AIMs reduced the exciton quenching caused by defect sites on the ZnO surface and enhanced the radiative decay of excitons.[27,31] The exciton lifetimes and PL intensities of SY on the ZnO subjected to AIMs increased with increasing number of amine groups in AIMs, which caused a decrease in the number of defect sites. The PL spectra of ZnO also showed that the peak centered at approximately 510 nm, which is well known as the green luminance of ZnO defects that is generally caused by oxygen vacancies,[54,55] and the peak attributed to the defect sites was suppressed by AIMs of the ZnO; a larger number of amine groups resulted in a larger number of reduced defect sites of ZnO.

The luminance and device efficiencies of iPLEDs with AIMs are significantly higher than those of the control devices, whereas the turn-on voltage (at 0.1 cd m^{-2}) of the iPLEDs with AIMs is less than that of the reference device, as shown in Figure 2b–d. Thus, AIM on the ZnO layer reduces the electron injection barrier between the ZnO and the SY by spontaneous negative dipolar polarization, as confirmed by ultraviolet photoelectron spectroscopy (UPS) measurements (see below **Figure 4**). As the number of amine groups of AIMs was increased from 2 to 6, the WFs of the ZnO/AIMs gradually decreased from 4.08 to 3.78 eV because of the strong interfacial dipole caused by the large number of amine groups in AIMs. Thus, the luminance and device efficiencies of iPLEDs gradually increase because the energy barriers gradually decrease with increasing number of amine groups in AIMs (see Figure S3a, Supporting Information).

Adv. Mater. **2015**,
DOI: 10.1002/adma.201500663

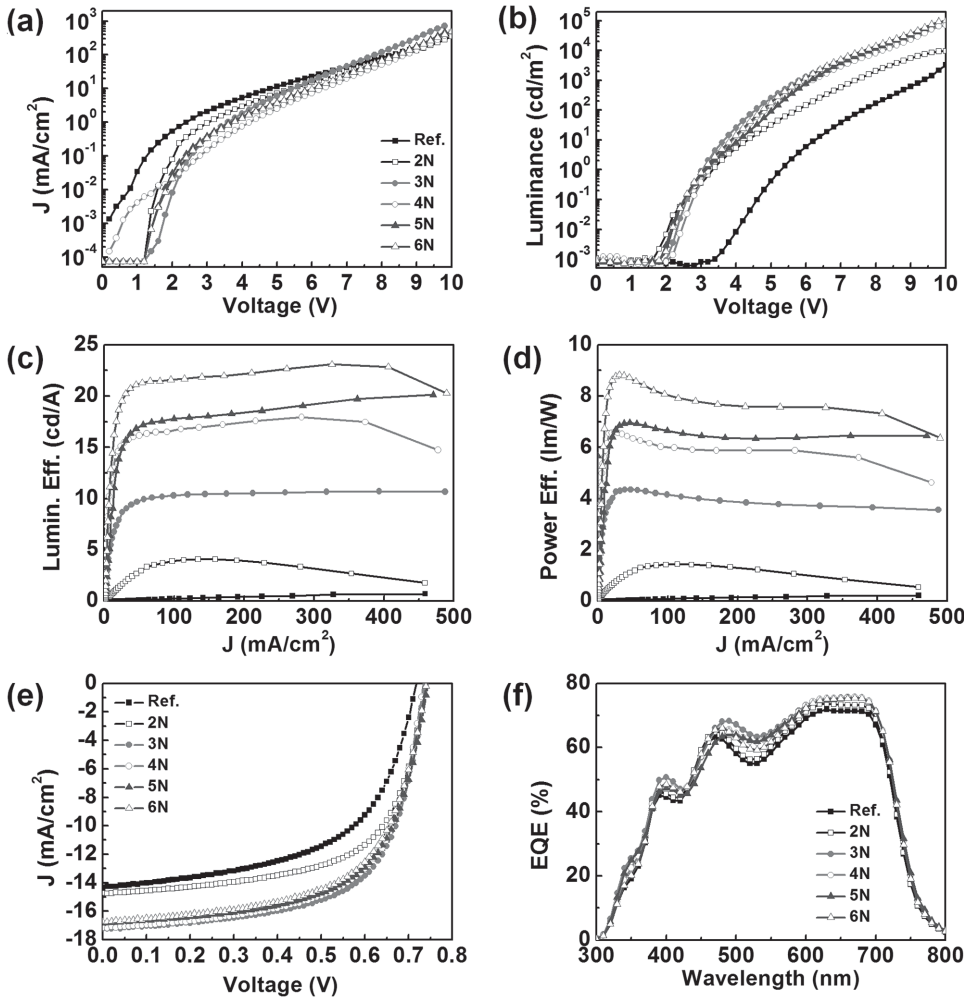

Figure 2. Performance of iPLEDs and iOSCs with AIMs. a) *J–V*, b) *L–V*, c) LE–*J*, and d) PE–*J* characteristics of iPLEDs. e) *J–V* characteristics and f) EQE characteristics of iOSCs under 1000 W m^{-2} AM 1.5G illumination.

This trend is consistent with electron-only device analysis (see Figure S4, Supporting Information). Electron-only devices with AIMs produced significantly higher current density compared to the reference device. As the number of amine groups in AIMs was increased, the electron current densities gradually increased because of the reduction of the injection barrier, which indicates more efficient electron injection. Among iPLEDs with AIMs, the optimized devices with PEHA (6N) exhibited a maximum luminance of 99 300 cd m^{-2}, a luminous efficiency (LE) of 23.1 cd A^{-1}, a power efficiency (PE) of 8.83 lm W^{-1} and an external quantum efficiency (EQE) of 8.40% because of its highest electron injection, reduction of leakage current and suppression of exciton quenching by passivation of defect sites on ZnO. The detailed performances of iPLEDs with and without AIMs are summarized in **Table 1**.

Figure 2e shows the *J–V* characteristics of iOSCs with and without AIMs for 1000 W m^{-2} air mass 1.5 global (AM 1.5G) illumination; the detailed device characteristics are summarized in Table 1. The iOSC device without AIMs exhibited substantially low device performance, such as a short-circuit current density (J_{sc}) of 14.35 mA cm^{-2}, an open-circuit voltage (V_{oc}) of 0.72 V, a fill factor (FF) of 0.67 and a power conversion efficiency (PCE) of 6.92%. Conversely, the iOSCs with AIMs showed remarkably enhanced PCEs compared to the control device. Optimized devices with DETA (3N) on the ZnO exhibited the highest PCE of 9.04%, which was enhanced by ≈30% compared to the PCE of the reference device. The EQE spectra of iOSCs in Figure 2f support an increase in PCE in the case of AIMs. The improved device performance originates from a reduction of defect sites on the ZnO surface and from the well-matched energy levels. The *J–V* characterizations of iOSCs in the dark also support the hypothesis that AIMs can reduce the defect sites on the ZnO surface (see Figure S5, Supporting Information). The dark current densities of iOSCs with AIMs are significantly smaller than those of the control device with reverse bias, which indicates reduced leakage current.

The energy diagrams of iOSCs are shown in Figure S3b, Supporting Information. The DETA (3N) already forms Ohmic contact by matching the energy level at the interface between the CB of ZnO (3.96 eV) and the LUMO of $PC_{71}BM$ (4.00 eV), which causes a reduced series resistance and efficient electron extraction. However, the surfaces of the ZnO with AIMs are

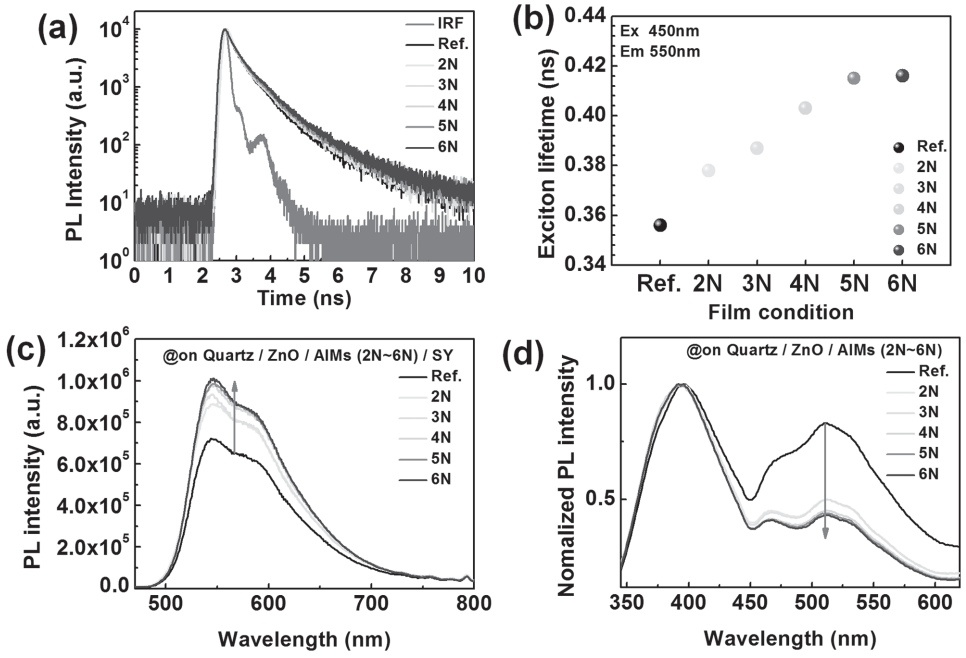

Figure 3. Exciton lifetime and PL intensity. a) Time-resolved PL signal of quartz/ZnO/SY with and without AIMs, as measured via TCSPC at 450 nm excitation. An emission wavelength is 550 nm. b) Summarized exciton lifetimes of SY on the ZnO with and without AIMs. c) PL spectra of quartz/ZnO/SY with and without AIMs at 470 nm excitation. d) PL spectra of quartz/ZnO with and without AIMs at 325 nm excitation.

more hydrophilic with an increase in the number of amine groups of AIMs because hydrophilic end groups tend to be oriented upward with the number of amine groups of AIMs, which results in poor compatibility between the ZnO and the hydrophobic active layer, as confirmed by contact angle measurements (see Figure S6, Supporting Information). Thus, iOSCs with DETA (3N) exhibited optimized device performance because of the well-matched energy level and relatively reasonable compatibility at the interface between the ZnO and the active layer.

The morphology of the ZnO surfaces with AIMs was not significantly altered, whereas the root-mean-square (rms) roughness values of the ZnO surfaces with AIMs slightly decreased compared with the roughness values without AIMs, which was confirmed by atomic force microscopy (AFM) (see Figure S7, Supporting Information).

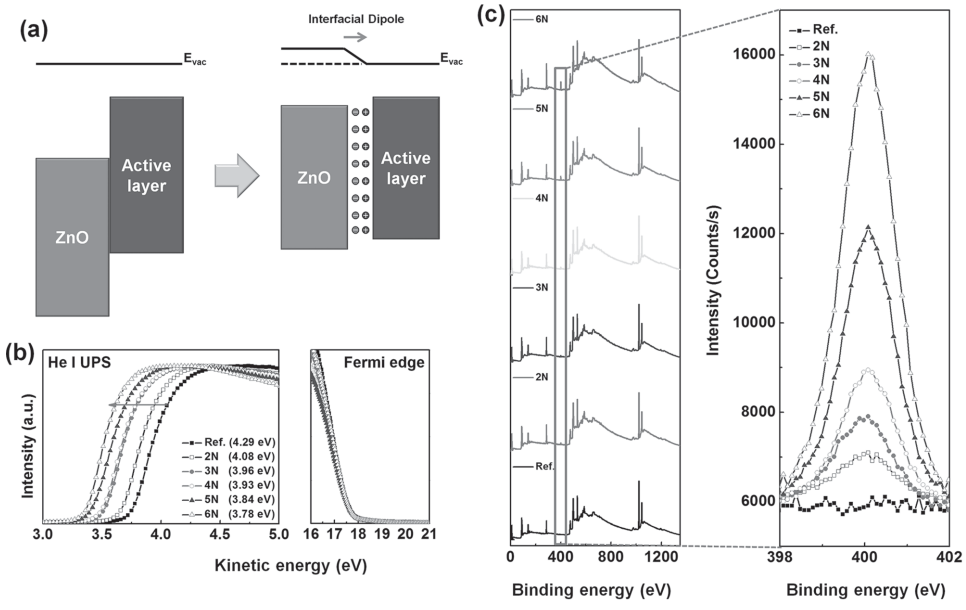

Figure 4. UPS and XPS analysis. a) Energy diagrams for flat band conditions at the ZnO/active layer with (right) and without (left) AIMs. b) UPS measurement and c) XPS measurement of ZnO with and without AIMs. The inset shows a high-resolution figure of the N1s peak.

Adv. Mater. **2015**,
DOI: 10.1002/adma.201500663

Table 1. Summarized device performance for iPLEDs and iOSCs with AIM.

Device configuration (iPLEDs)	L_{max} [cd m^{-2}]@bias	LE_{max} [cd A^{-1}]@bias	PE_{max} [lm W^{-1}]@bias	EQE_{max} [%]@bias	Turn-on voltage [V]@0.1 cd m^{-2}
ITO/ZnO/SY/MoO_3/Au	3,320 ± 150 (10.0 V)	0.723 ± 0.030 (10.0 V)	0.227 ± 0.012 (10.0 V)	0.281 ± 0.008 (10.0 V)	4.6
ITO/ZnO/2-ME+EDA (2N)/SY/MoO_3/Au	9,500 ± 200 (10.0 V)	4.10 ± 0.25 (9.0 V)	1.44 ± 0.15 (8.8 V)	1.55 ± 0.13 (9.0 V)	2.6
ITO/ZnO/2-ME+DETA (3N)/SY/MoO_3/Au	66,570 ± 450 (9.8 V)	10.7 ± 0.8 (9.2 V)	4.35 ± 0.24 (7.0 V)	4.13 ± 0.15 (8.0 V)	2.6
ITO/ZnO/2-ME+TETA (4N)/SY/MoO_3/Au	70,410 ± 560 (10.0 V)	18.0 ± 1.2 (9.6 V)	6.59 ± 0.40 (7.2 V)	6.57 ± 0.30 (9.6 V)	2.8
ITO/ZnO/2-ME+TEPA (5N)/SY/MoO_3/Au	94,650 ± 620 (9.8 V)	20.1 ± 0.9 (9.8 V)	6.96 ± 0.45 (7.6 V)	7.20 ± 0.36 (9.6 V)	2.6
ITO/ZnO/2-ME+PEHA (6N)/SY/MoO_3/Au	99, 290 ± 650 (10.0 V)	23.1 ± 1.0 (9.6 V)	8.83 ± 0.52 (7.2 V)	8.40 ± 0.42 (8.0 V)	2.6
Device configuration (iOSCs)		J_{sc} [mA cm^{-2}]	V_{oc} [V]	*FF*	η [%]
ITO / ZnO / PTB7:PC_{71}BM / MoO_3 / Ag		14.35 ± 0.14	0.72 ± 0.01	0.67 ± 0.01	6.92 ± 0.12
ITO/ZnO/2-ME+EDA (2N)/PTB7:PC_{71}BM / MoO_3/Ag		14.72 ± 0.12	0.74 ± 0.01	0.70 ± 0.01	7.62 ± 0.09
ITO/ZnO/2-ME+DETA (3N)/PTB7:PC_{71}BM / MoO_3/Ag		17.21 ± 0.13	0.74 ± 0.01	0.71 ± 0.01	9.04 ± 0.11
ITO/ZnO/2-ME+TETA (4N)/PTB7:PC_{71}BM / MoO_3/Ag		17.18 ± 0.17	0.74 ± 0.01	0.71 ± 0.01	9.03 ± 0.15
ITO/ZnO/2-ME+TEPA (5N)/PTB7:PC_{71}BM/MoO_3/Ag		16.84 ± 0.15	0.74 ± 0.01	0.68 ± 0.01	8.47 ± 0.14
ITO/ZnO/2-ME+PEHA (6N)/PTB7:PC_{71}BM/MoO_3/Ag		16.73 ± 0.12	0.74 ± 0.01	0.68 ± 0.01	8.42 ± 0.10

The total number of amine groups in solutions was fixed to observe the effect of the number of amine groups in one molecule on the energy level tuning process (see Table S2, Supporting Information). When the number of amine groups on the surface of ZnO was increased, the WFs of ZnO with AIMs were further reduced, even when the total number of amine groups was fixed, as shown in Figure 4a.

To understand the possible origin of the reduction of WFs, depending on the number of amine groups on the surface of the ZnO layer, quantitative X-ray photoelectron spectroscopy (XPS) analysis (Figure 4b) was conducted. The total number of amine groups in AIMs solution was fixed, as shown in Table S2, Supporting Information. Zhou et al. demonstrated that neutral amine groups on the surface of ZnO contributed to the interface dipole, which caused significant changes in WFs.[26] The reduction in the WFs of ZnO upon AIMs is attributed to the interface dipole induced by electron transfer from the nitrogen of the amine groups to the zinc of ZnO. The survey XPS spectra of the ZnO with AIMs exhibited an N1s peak at a binding energy of approximately 400 eV. In the N1s peaks in the high-resolution XPS spectra, two asymmetric N1s peaks can be assigned to a N–C peak (400.1 eV) and a N–Zn peak (398.8 eV)[31,32,56–58] (see Figure S8, Supporting Information). The total intensities of N1s peaks and N–Zn increased along with the number of amine groups in AIM. It means that the probability of amine group adsorption on the ZnO surface increases with the number of amine group and the amount of remaining AIM after the annealing is influenced by molecular weights ($\bar{M}_w$) of AIM due to different vapor pressure. This observation suggests that AIM with a larger number of amine groups passivated more defect sites and induced a stronger interface dipole, which eventually caused a greater reduction in the WF. On the basis of the evidence collected from the XPS spectra and the contact angle measurements, we argue that the number of nitrogen atoms in AIMs plays a crucial role in the conformation of AIMs in modulating the surface properties of the ZnO. For example, with an increase in the number of nitrogen atoms adsorbed onto the ZnO surfaces, the fraction of the hydrophobic ethylene backbone that is not bound to the surface may increase and result in a greater number of hydrophobic surfaces. However, as the number of amine groups in AIM increases, the number of nonadsorbed nitrogen may also increase, as shown in Figure S9, Supporting Information. Schematic illustrations of the ZnO surfaces with AIM of (a) EDA (2N), (c) DETA (3N), and (e) PEHA (6N) were represented. There are various conformations of AIM on the ZnO surface. Each example of the conformations of (a,b) EDA (2N), (c,d) DETA (3N), and (e,f) PEHA (6N) was illustrated.

Moreover, the stability of optimized iPLEDs and iOSCs with AIM was measured under an ambient air condition with encapsulation for minimizing the degradation of top electrode, as shown in Figure S10, Supporting Information. In specific, various parameters of best performing iPLEDs and iOSCs with respective AIM treatment were evaluated for 5 d, exhibiting excellent stability without altering values from initial states. Furthermore, our group has already demonstrated the excellent long-term stability of iPLEDs and iOSCs with similar type of AIMs such as 2-methoxyethanol and ethanolamine (2-ME+EA).[32,59]

In summary, we demonstrated highly efficient iPLEDs and iOSCs by employing AIMs as a versatile interlayer, which comprises a simple, inexpensive and effective method. AIMs that can tune energy levels at the interface between the ZnO and the active layer via use of AIMs with different numbers of amine groups effectively decreases the energy barrier between the ZnO and the active layer, passivates the defect sites of the ZnO and blocks the holes, which enhances the device performance of both iPLEDs and iOSCs. Optimized iPLEDs with PEHA (6N) exhibit a maximum luminance of 99 300 cd m^{-2}, a LE of 23.1 cd A^{-1}, a PE of 8.83 lm W^{-1}, and an EQE of 8.40%, which are enhanced ≈30-, 32-, 38-, and 30-fold, respectively, compared to the reference device. For iOSCs, optimized iOSCs with DETA (3N) exhibited a PCE of 9.04%, which is enhanced by approximately 30% compared to the reference devices. Our approach is

therefore a promising method for obtaining high device performance in organic-based optoelectronic devices.

Experimental Section

Preparation of ZnO Film: The ZnO solutions of 0.75 and 0.50 M were prepared by dissolving zinc acetate dehydrate [$Zn(CH_3COO)_2{\cdot}2H_2O$] in 2-ME and EA cosolvents for iPLED devices and iOSC devices, respectively. The details are described elsewhere.[31]

Preparation of AIMs: AIMs solutions that contain 2 to 6 amine groups (2 to 6N) at concentrations of 0.30 and 0.06 M for iPLED and iOSC devices, respectively, were prepared by dilution of the amines in 2-ME. Subsequently, AIMs precursor solutions were spin-cast at 3000 rpm onto the ZnO surface and then annealed at 120 °C for 10 min.

iPLEDs and iOSCs Fabrication: The ZnO layer was spin-coated onto ITO substrates that had been previously subjected to a 20 min UV-ozone treatment, and the coated substrates were then heated at 400 °C for 20 min. Subsequently, AIMs were spin-cast onto the ZnO layer at 3000 rpm on the ZnO surface and then annealed at 120 °C for 10 min under ambient atmosphere.

For iPLEDs, poly(phenyl vinylene):SY (Merck Co., $\bar{M}_w = 1\,950\,000$ g mol^{-1}) solution dissolved in chlorobenzene (0.6 wt%) was spin-coated at 2000 rpm for 45 s onto AIMs/ZnO for the emissive layer. MoO_3 (10 nm) and Au (100 nm) were thermally evaporated onto the SY under vacuum conditions (<10^{-6} Torr) with a slow deposition rate of 0.03 nm s^{-1}.

For iOSCs, a PTB7 (1-Material Co.) and $PC_{71}BM$ (Rieke Metal Co.) blending solution dissolved in a mixed solvent of chlorobenzene and 1,8-diiodoctane (97:3% by volume) (concentration, 25 mg mL^{-1}) was spin-coated at 800 rpm for 60 s onto AIMs/ZnO for the active layer. MoO_3 (5 nm) and Ag (100 nm) were thermally evaporated onto the active layer under vacuum conditions (<10^{-6} Torr) with a slow deposition rate of 0.03 nm s^{-1}. The area of the device was 13.0 mm^2.

iPLEDs and iOSCs Characterization: For iPLEDs, the *J–V–L* characteristics and device performances were measured using a Konica Minolta spectroradiometer (CS-2000) with Keithley 2400 source meter, respectively. For iOSCs, *J–V* characteristics and PCE measurements were performed using an IviumStat source meter (Ivium Technologies, Eindhoven) and a solar simulator (Portable Solar Simulator PEC-L01, Peccell Technologies, Inc., Kanagawa) with 1000 W m^{-2} AM 1.5G illumination.

TCSPC Analysis: The exciton lifetime was observed using the TCSPC method. The details are described elsewhere.[60]

Supporting Information

Supporting Information is available from the Wiley Online Library or from the author.

Acknowledgements

B.R.L. and S.L. contributed equally to this work. This study was supported by the Mid-Career Researcher Program (2012R1A2A2A06046931). This work was financially supported by the KIST-UNIST partnership program (UNIST, 2.140441.01/2.140442.01) or equivalently by the 2014 Research Fund (1.140019.01) of UNIST (Ulsan National Institute of Science and Technology). This work was supported by the National Research Foundation of Korea (NRF) under Grant No. 2014R1A2A1A11052829.

Received: February 7, 2015
Revised: April 12, 2015
Published online:

[1] J. H. Burroughes, D. D. C. Bradley, A. R. Brown, R. N. Marks, K. Mackay, R. H. Friend, P. L. Burn, A. B. Holmes, *Nature* **1990**, *347*, 539.
[2] R. H. Friend, R. W. Gymer, A. B. Holmes, J. H. Burroughes, R. N. Marks, C. Taliani, D. D. C. Bradley, D. A. Dos Santos, J. L. Bredas, M. Logdlund, W. R. Salaneck, *Nature* **1999**, *397*, 121.
[3] M. S. White, M. Kaltenbrunner, E. D. Glowacki, K. Gutnichenko, G. Kettlgruber, I. Graz, S. Aazou, C. Ulbricht, D. A. M. Egbe, M. C. Miron, Z. Major, M. C. Scharber, T. Sekitani, T. Someya, S. Bauer, N. S. Sariciftci, *Nat. Photonics* **2013**, *7*, 811.
[4] B. R. Lee, J. S. Kim, Y. S. Nam, H. J. Jeong, S. Y. Jeong, G.-W. Lee, J. T. Han, M. H. Song, *J. Mater. Chem.* **2012**, *22*, 21481.
[5] G. Yu, J. Gao, J. C. Hummelen, F. Wudl, A. J. Heeger, *Science* **1995**, *270*, 1789.
[6] J. Y. Kim, K. Lee, N. E. Coates, D. Moses, T. Q. Nguyen, M. Dante, A. J. Heeger, *Science* **2007**, *317*, 222.
[7] G. Li, R. Zhu, Y. Yang, *Nat. Photonics* **2012**, *6*, 153.
[8] S.-J. Ko, H. Choi, W. Lee, T. Kim, B. R. Lee, J.-W. Jung, J.-R. Jeong, M. H. Song, J. C. Lee, H. Y. Woo, J. Y. Kim, *Energy Environ. Sci.* **2013**, *6*, 1949.
[9] K. Lee, J. Y. Kim, S. H. Park, S. H. Kim, S. Cho, A. J. Heeger, *Adv. Mater.* **2007**, *19*, 2445.
[10] S. K. Hau, H.-L. Yip, N. S. Baek, J. Zou, K. O'Malley, A. K. Y. Jen, *Appl. Phys. Lett.* **2008**, *92*, 253301.
[11] M. S. Weaver, L. A. Michalski, K. Rajan, M. A. Rothman, J. A. Silvernail, J. J. Brown, P. E. Burrows, G. L. Graff, M. E. Gross, P. M. Martin, M. Hall, E. Mast, C. Bonham, W. Bennett, M. Zumhoff, *Appl. Phys. Lett.* **2002**, *81*, 2929.
[12] K. Morii, M. Ishida, T. Takashima, T. Shimoda, Q. Wang, M. K. Nazeeruddin, M. Graetzel, *Appl. Phys. Lett.* **2006**, *89*, 183510.
[13] K. Morii, T. Kawase, S. Inoue, *Appl. Phys. Lett.* **2008**, *92*, 213304.
[14] H. J. Bolink, E. Coronado, J. Orozco, M. Sessolo, *Adv. Mater.* **2009**, *21*, 79.
[15] T.-W. Lee, J. Hwang, S.-Y. Min, *ChemSusChem* **2010**, *3*, 1021.
[16] A. K. K. Kyaw, X. W. Sun, C. Y. Jiang, G. Q. Lo, D. W. Zhao, D. L. Kwong, *Appl. Phys. Lett.* **2008**, *93*, 221107.
[17] J. B. You, C. C. Chen, L. T. Dou, S. Murase, H. S. Duan, S. A. Hawks, T. Xu, H. J. Son, L. P. Yu, G. Li, Y. Yang, *Adv. Mater.* **2012**, *24*, 5267.
[18] F. Zhang, X. Xu, W. Tang, J. Zhang, Z. Zhuo, J. Wang, J. Wang, Z. Xu, Y. Wang, *Sol. Energy Mater. Sol. Cells* **2011**, *95*, 1785.
[19] J. S. Park, B. R. Lee, J. M. Lee, J.-S. Kim, S. O. Kim, M. H. Song, *Appl. Phys. Lett.* **2010**, *96*, 243306.
[20] H. Ma, H.-L. Yip, F. Huang, A. K. Y. Jen, *Adv. Funct. Mater.* **2010**, *20*, 1371.
[21] B. R. Lee, H. Choi, J. S. Park, H. J. Lee, S. O. Kim, J. Y. Kim, M. H. Song, *J. Mater. Chem.* **2011**, *21*, 2051.
[22] H. Choi, J. S. Park, E. Jeong, G.-H. Kim, B. R. Lee, S. O. Kim, M. H. Song, H. Y. Woo, J. Y. Kim, *Adv. Mater.* **2011**, *23*, 2759.
[23] B. R. Lee, W. Lee, N. Thanh Luan, J. S. Park, J.-S. Kim, J. Y. Kim, H. Y. Woo, M. H. Song, *ACS Appl. Mater. Interfaces* **2013**, *5*, 5690.
[24] B. H. Lee, I. H. Jung, H. Y. Woo, H.-K. Shim, G. Kim, K. Lee, *Adv. Funct. Mater.* **2014**, *24*, 1100.
[25] H. Kang, S. Hong, J. Lee, K. Lee, *Adv. Mater.* **2012**, *24*, 3005.
[26] Y. Zhou, C. Fuentes-Hernandez, J. Shim, J. Meyer, A. J. Giordano, H. Li, P. Winget, T. Papadopoulos, H. Cheun, J. Kim, M. Fenoll, A. Dindar, W. Haske, E. Najafabadi, T. M. Khan, H. Sojoudi, S. Barlow, S. Graham, J.-L. Bredas, S. R. Marder, A. Kahn, B. Kippelen, *Science* **2012**, *336*, 327.
[27] Y.-H. Kim, T.-H. Han, H. Cho, S.-Y. Min, C.-L. Lee, T.-W. Lee, *Adv. Funct. Mater.* **2014**, *24*, 3808.
[28] S. Woo, W. H. Kim, H. Kim, Y. Yi, H.-K. Lyu, Y. Kim, *Adv. Energy Mater.* **2014**, *4*, 1301692.
[29] Z. He, C. Zhong, S. Su, M. Xu, H. Wu, Y. Cao, *Nat. Photonics* **2012**, *6*, 591.

[30] L. P. Lu, D. Kabra, R. H. Friend, *Adv. Funct. Mater.* **2012**, *22*, 4165.
[31] B. R. Lee, E. D. Jung, J. S. Park, Y. S. Nam, S. H. Min, B.-S. Kim, K.-M. Lee, J.-R. Jeong, R. H. Friend, J. S. Kim, S. O. Kim, M. H. Song, *Nat. Commun.* **2014**, *5*, 5840.
[32] B. R. Lee, E. D. Jung, Y. S. Nam, M. Jung, J. S. Park, S. Lee, H. Choi, S.-J. Ko, N. R. Shin, Y.-K. Kim, S. O. Kim, J. Y. Kim, H.-J. Shin, S. Cho, M. H. Song, *Adv. Mater.* **2014**, *26*, 494.
[33] D. R. Gagnon, J. D. Capistran, F. E. Karasz, R. W. Lenz, S. Antoun, *Polymer* **1987**, *28*, 567.
[34] Y. He, S. Gong, R. Hattori, J. Kanicki, *Appl. Phys. Lett.* **1999**, *74*, 2265.
[35] H. J. Song, S. M. Lee, J. Y. Lee, B. H. Choi, D. K. Moon, *Synth. Met.* **2011**, *161*, 2451.
[36] Y. J. Cheng, S. H. Yang, C. S. Hsu, *Chem. Rev.* **2009**, *109*, 5868.
[37] M. P. Nikiforov, B. Lai, W. Chen, S. Chen, R. D. Schaller, J. Strzalka, J. Maser, S. B. Darling, *Energy Environ. Sci.* **2013**, *6*, 1513.
[38] Y. Liang, Z. Xu, J. Xia, S.-T. Tsai, Y. Wu, G. Li, C. Ray, L. Yu, *Adv. Mater.* **2010**, *22*, E135.
[39] L. Ye, S. Zhang, L. Huo, M. Zhang, J. Hou, *Acc. Chem. Res.* **2014**, *47*, 1595.
[40] S. Zhang, L. Ye, W. Zhao, D. Liu, H. Yao, J. Hou, *Macromolecules* **2014**, *47*, 4653.
[41] Y. Nakayama, K. Morii, Y. Suzuki, H. Machida, S. Kera, N. Ueno, H. Kitagawa, Y. Noguchi, H. Ishii, *Adv. Funct. Mater.* **2009**, *19*, 3746.
[42] M. Kroeger, S. Hamwi, J. Meyer, T. Riedl, W. Kowalsky, A. Kahn, *Appl. Phys. Lett.* **2009**, *95*, 123301.
[43] Y. Liu, C.-C. Chen, Z. Hong, J. Gao, Y. Yang, H. Zhou, L. Dou, G. Li, Y. Yang, *Sci. Rep.* **2013**, *3*, 3356.
[44] J. You, L. Dou, K. Yoshimura, T. Kato, K. Ohya, T. Moriarty, K. Emery, C.-C. Chen, J. Gao, G. Li, Y. Yang, *Nat. Commun.* **2013**, *4*, 1466.
[45] L. Dou, J. You, J. Yang, C.-C. Chen, Y. He, S. Murase, T. Moriarty, K. Emery, G. Li, Y. Yang, *Nat. Photonics* **2012**, *6*, 180.
[46] S. Yamakawa, K. Tajima, K. Hashimoto, *Org. Electronics* **2009**, *10*, 511.
[47] S. K. Hau, H.-L. Yip, O. Acton, N. S. Baek, H. Ma, A. K. Y. Jen, *J. Mater. Chem.* **2008**, *18*, 5113.
[48] S. K. Hau, H.-L. Yip, H. Ma, A. K. Y. Jen, *Appl. Phys. Lett.* **2008**, *93*, 233304.
[49] H. Ma, H. L. Yip, F. Huang, A. K. Y. Jen, *Adv. Funct. Mater.* **2010**, *20*, 1371.
[50] H.-L. Yip, A. K. Y. Jen, *Energy Environ. Sci.* **2012**, *5*, 5994.
[51] T. Yang, M. Wang, C. Duan, X. Hu, L. Huang, J. Peng, F. Huang, X. Gong, *Energy Environ. Sci.* **2012**, *5*, 8208.
[52] S. R. Cowan, A. Roy, A. J. Heeger, *Phys. Rev. B* **2010**, *82*, 245207.
[53] X. Gong, M. Tong, F. G. Brunetti, J. Seo, Y. Sun, D. Moses, F. Wudl, A. J. Heeger, *Adv. Mater.* **2011**, *23*, 2272.
[54] G. Xiong, U. Pal, J. G. Serrano, K. B. Ucer, R. T. Williams, *Phys. Status Solidi C* **2006**, *10*, 3577.
[55] K. Vanheusden, W. L. Warren, C. H. Seager, D. R. Tallant, J. A. Voigt, B. E. Gnade, *J. Appl. Phys.* **1996**, *79*, 7983.
[56] G. Jayalakshmi, N. Gopalakrishnan, T. Balasubramanian, *J. Alloys Compd.* **2013**, *551*, 667.
[57] T. M. Barnes, J. Leaf, S. Hand, C. Fry, C. A. Wolden, *J. Appl. Phys.* **2004**, *96*, 7036.
[58] H. Maki, I. Sakaguchi, N. Ohashi, S. Sekiguchi, H. Haneda, J. Tanaka, N. Ichinose, *Jpn. J. Appl. Phys.* **2003**, *42*, 75.
[59] B. R. Lee, J.-W. Kim, D. Kang, D. W. Lee, S.-J. Ko, H. J. Lee, C.-L. Lee, J. Y. Kim, H. S. Shin, M. H. Song, *ACS Nano* **2012**, *6*, 2984.
[60] S. Lee, B. R. Lee, J. S. Kim, M. H. Song, *J. Mater. Chem C* **2014**, *2*, 8673.